$5d$-level energies of Ce^{3+} and the crystalline environment. I. Fluoride compounds

P. Dorenbos
Interfaculty Reactor Institute, Delft University of Technology, Mekelweg 15, 2629 JB Delft, The Netherlands
(Received 28 June 2000)

Information on the position of all five $5d$ levels of Ce^{3+} in 17 different fluoride compounds has been collected. A model involving the polarizability of the fluoride ions, originally suggested by Morrison [J. Chem. Phys. **72**, 1001 (1980)], is used to calculate the so-called spectroscopic polarizability α_{sp} from the observed average energy of the $5d$ configuration. It will be compared with actual in-crystal fluoride ion polarizabilities. There appears a relationship between α_{sp} and the types of cations present in the crystal structure. Small high valency cations tend to reduce the centroid shift. Large cations have the opposite effect. The size and the type of the fluoride ion coordination polyhedron around Ce^{3+} determine the crystal field splitting of the $5d$ levels. Combining the gained knowledge on centroid shift and crystal field splitting, the energy of the first $4f \rightarrow 5d$ transition in about 25 additional fluoride compounds will be interpreted.

I. INTRODUCTION

The present paper forms part of a series of papers in which the fd transitions of the trivalent lanthanides in inorganic crystalline compounds is the subject of study. In Ref. 1, the crystal field depression or spectroscopic redshift $D(A)$ was defined. It expresses the amount by which the energy of the first dipole-allowed fd transition is lowered whenever the lanthanide ion is doped in a host crystal. Experimental data reveal that, when doped in the same host crystal, this redshift in first approximation is the same for all 13 trivalent lanthanides.[1] This provides large predictive potential. If the redshift is known for just one of the lanthanides, the first allowed $4f^n \rightarrow 4f^{n-1}5d$ transition of all others can be estimated.

Apart from possibly Eu^{2+}, most scientific papers on $4f$-$5d$ spectroscopy deal with Ce^{3+} in a crystalline host. The ground-state configuration contains one single optically active electron in the well-shielded $4f$ shell. It can be excited to the $5d$ configuration and, depending on the site symmetry, at most five distinct $4f \rightarrow 5d$ transitions can be observed. Due to the interaction with the crystal field, the average position of the $5d$ levels, i.e., the centroid or barycenter, is lowered relative to the position for the free ion. This combined with the crystal field and spin-orbit splitting results in a redshift of the first $4f \rightarrow 5d$ transition. $D(A)$ can be written as

$$D(A) = [E_c(\text{free}) - E_c(A)] + [\epsilon_s(A) - \epsilon_s(\text{free})]$$
$$= \epsilon_c(A) + \epsilon_s(A) - 1890 \ \text{cm}^{-1}, \quad (1)$$

where $E_c(\text{free}) = 51\,230 \ \text{cm}^{-1}$ is the centroid position of Ce^{3+} as a free ion[2] and $E_c(A)$ likewise for Ce in compound A. The difference $\epsilon_c(A)$ will be called here the centroid shift. $\epsilon_s(\text{free}) = 1890 \ \text{cm}^{-1}$ is the energy difference between centroid position and the lowest $5d$ level ($^2D_{3/2}$) of the free Ce^{3+} ion. $\epsilon_s(A)$ likewise if doped in host A. It represents the contribution to the redshift due to crystal field and spin-orbit splitting. This contribution will be called the crystal field shift.

It is more convenient to interpret the total splitting, defined as the difference between the lowest and highest $5d$ level, instead of the crystal field shift. Although both spin-orbit and crystal field splitting will contribute, it will hereafter be referred to as the crystal field splitting ϵ_{cfs}. Equation (1) is rewritten as

$$D(A) = \epsilon_c(A) + \frac{\epsilon_{cfs}(A)}{r(A)} - 1890 \ \text{cm}^{-1}, \quad (2)$$

where $r(A)$ expresses the ratio between crystal field splitting and crystal field shift.

Values for $D(A)$ belonging to 350 different sites in over 300 different compounds have been compiled in Ref. 3. In order to display and analyze these data in a systematic way, a seven-digit identification number was assigned to each of the compounds. By treating this number as a variable A, the redshift $D(A)$ can be displayed, as is done in Fig. 1. On the scale in Fig. 1 only the first two digits are of significance. They are representative of the types of anions in the host

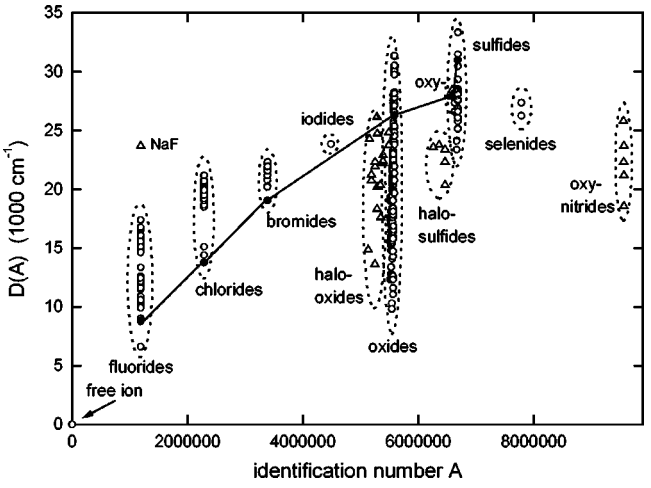

FIG. 1. The spectroscopic redshift $D(A)$ of the trivalent lanthanides in inorganic compounds (from Ref. 3). The solid line connects data points belonging to LaF_3, $LaCl_3$, $LaBr_3$, La_2O_3, La_2O_2S, and La_2S_3.

crystal. Notice the grouping of the data into the fluorides, chlorides, bromides, iodides, oxides, sulfides, selenides, tellurides (no data available), and nitrides. The redshift varies from the lowest value of 6600 cm^{-1} for $KMgF_3$ to the largest value of 33 300 cm^{-1} for $MgSc_2S_4$. In the case of Ce^{3+}, this corresponds with 234 nm and 625 nm for the first fd absorption band, respectively.

The purpose of this and following papers is to study how centroid shift, crystal field splitting, and redshift are related to the crystalline environment. The data will be interpreted with the aim to find clear trends. Once the trends are firmly established, not only qualitatively but also quantitatively, they can be used to predict 5d-level positions of the lanthanides in yet uninvestigated materials. The established trends may also help in guiding theoretical modelings. In this paper (Part I) the 5d-level positions of Ce^{3+} when doped in fluoride compounds are studied. In the accompanying paper (Part II) the chlorides, bromides, and iodides are treated. Since this is the first in a planned series of papers, crystal field theory applied to 5d levels and some phenomenological models will be briefly reviewed.

A model involving the polarizability of the fluoride ions will be developed that appears quite successful in revealing the trends in the centroid shift with the crystalline environment. The crystal field splitting behaves quite independently from the centroid shift. It is controlled by the size and shape of the fluoride ion polyhedron coordinating the Ce^{3+} ion. After the interpretation of the centroid shift and crystal field splitting of 17 different compounds, the total redshift of the full collection of about 40 different fluoride materials will be interpreted.

II. MODELS ON CRYSTAL FIELD INTERACTION

The most simple form of crystal field theory is the point charge electrostatic model (PCEM). Each anion that coordinates the metal ion is represented by a monopole having the valency value of the anion. They produce a crystal field consisting of a spherically symmetric part and a nonspherical part; see, for example, Ref. 4. The interaction of the nonspherical part with the 5d electron causes the crystal field splitting. A comprehensive review of the PCEM can be found in the work by Görller-Walrand and Binnemans.[5]

A limitation of *ionic models* like the PCEM is their inability to predict any centroid shift. Yet, experimentally it is observed that in a crystal, the average energy of an LS term of the $4f^n$ configuration of a lanthanide ion is lower than the free ion value.[6] The same holds for the d^n levels of the transition-metal ions and the 5d configuration of the lanthanides. The amount of lowering, i.e., centroid shift, tends to increase with the reducing character (electron donating power) of the nearest-neighbor anions in the order

$$F^- < Cl^- < Br^- < I^- < O^{2-} < S^{2-}, \tag{3}$$

which is known as the nephelauxetic series (see Chap. 23 in Ref. 7). Note that the same ordering can be seen for the spectroscopic redshift of the La-based compounds in Fig. 1.

The centroid shift has a long time ago been attributed to an expansion of the charge cloud, i.e., the *nephelauxetic effect*.[7] It results in larger average distance and hence reduced Coulomb repulsion between the electrons of the metal (lanthanide) cation. Later, other theories were developed also. One of them is based on the quantum-mechanical overlap between metal and anion ligands causing antibonding and bonding orbitals. Sugano and Shulman[8] used such molecular orbital formalism in 1963, and showed that the $3d^8$ levels of Ni^{2+} in $KMgF_3$ are much influenced by these *covalency effects*. Morrison[9] was the first who suggested in 1980 a physical origin for the centroid shift involving *ligand polarization*. The instantaneous position of the metal electron polarizes the surrounding ligands, which react back on the metal electron itself. Essentially a self-induced potential is generated that reduces the interelectron Coulomb repulsion between the metal electrons. It leads, like the nephelauxetic effect, to a lowering of the centroid energy of the LS terms. Both the covalency model and the ligand polarization model were reviewed by Aull and Jenssen[10] in 1986 in order to formulate a model for the 5d-level spectroscopy of Ce^{3+}.

Theoretically, the Hamiltonian of the metal ion is often written as a sum of the free metal ion Hamiltonian and a single electron crystal field Hamiltonian containing the so-called B_q^k crystal field parameters.[5] The effects of charge cloud expansion, covalency, and ligand polarization are taken into account by adding correlation crystal field terms to the Hamiltonian.[11] The values for the crystal field and correlation parameters are obtained from the observed positions of the energy levels. The next step in understanding the crystal field interaction is to relate those phenomenologically determined parameters to the type of crystalline environment.

In this work the ligand polarization model as suggested by Morrison[9] will be further developed to analyze the centroid shift. Following Morrison[9] and Aull and Jenssen,[10] ϵ_c can in first approximation be written as

$$\epsilon_c = \frac{e^2}{4\pi\epsilon_0}(\langle r^2\rangle_{5d} - \langle r^2\rangle_{4f}) \sum_{i=1}^{N} \frac{\alpha_i}{R_i^6}, \tag{4}$$

where r represents the radial position of the electron in either the 5d or 4f orbital, and $\langle r^2\rangle$ is the expectation value of r^2, α_i is the polarizability of the ligand i located a distance R_i from the metal ion, e is the elementary charge, and ϵ_0 is the permittivity of vacuum. The summation is over all N nearest coordinating anion ligands. The ligand polarization model has, to the author's knowledge, only been used by Morrison to interpret the redshift in Ce^{3+}-doped fluoride crystals and by Aull and Jenssen[10] to interpret the centroid shift in several Ce^{3+}-doped elpasolite fluoride crystals.

Models on covalency predict in first order a centroid shift proportional to the square of the overlap integral $S \equiv \langle \phi_M | \psi_L \rangle$ between the metal (M) and ligand (L) orbital.[10,12] For the centroid shift one may write

$$\epsilon_c = \sum_{i=1}^{N} (a_i \langle \phi_{5d} | \psi_{L_i} \rangle^2 - b_i \langle \phi_{4f} | \psi_{L_i} \rangle^2), \tag{5}$$

where a_i and b_i are appropriate constants.

Caro and co-workers[13,14] and Antic-Fidancev *et al.*[15] systematically studied ff transitions in Nd^{3+}, Gd^{3+}, and Eu^{3+} in many different compounds. Caro and Derouet[13] relate the fractional centroid shift of Nd^{3+} $4f^3$ LS terms to the amount of overlap S between anion ligands and metal wave functions. Later in 1976 Caro *et al.*[14] suggest a possible relation-

ship with the polarizability of the lattice. In 1987 the situation on the centroid shift of the $^2P_{1/2}$ level of Nd^{3+} was reviewed by Antic-Fidancev *et al.*[15] A main conclusion was that a qualitative explanation of the centroid shift still had to be found. Denning *et al.*[11] demonstrate for the Tb^{3+} $4f^7$ levels in Cs_2NaTbX_6 ($X=F,Cl,Br$) that correlation crystal field terms in the Hamiltonian become increasingly more important in the order $F<Cl<Br$, which is the same ordering as in Eq. (3). It was attributed to either a large contribution from covalency or from ligand polarization or from a combination of both. The relative importance of these contributions was not known. Understanding the centroid shift of LS terms is still a challenging problem of $4f^n$-level spectroscopy.

The few systematic studies that have appeared on $5d$-level spectroscopy pertain to the lowest $5d$ level and not to the centroid shift. In 1967 Blasse and Bril reported on about 30 different Tb^{3+}-doped[16] and 20 different Ce^{3+}-doped[17] oxides. In 1976 Fouassier *et al.*[18] studied fd transitions in 13 different Eu^{2+}-doped $M_xB_yF_z$ fluoride compounds, where $M=Ca^{2+}$, Sr^{2+}, or Ba^{2+} and $B=Si^{4+}$, Y^{3+}, Be^{2+}, Mg^{2+}, or Li^+. Besides the fd transitions in over 20 different Eu^{2+}-doped compounds, van Uitert[19] in 1984 also studied about 9 different Ce^{3+}-doped compounds, not only in fluorides but also in some chloride, oxide, and sulfide systems.

It was noticed by Blasse and Bril[16] that the first electric dipole-allowed absorption in Tb^{3+}-doped $Y_2Ca_2Si_2O_9$, $Y_4Al_2O_9$, and $Y_4Ga_2O_9$ shifts from 235 nm to 253 nm to 268 nm. All three compounds have the same crystal structure. Replacing Si^{4+} by the larger Al^{3+} ion or by the even larger Ga^{3+} effects the electron clouds of the oxygen ions. Blasse and Bril suggested that they are less and less attracted (polarized) toward these larger cations. Fouassier *et al.*[18] observed essentially the same for the 13 Eu^{2+}-doped ternary fluoride compounds. In $BaSiF_6$ with Eu on the large Ba^{2+} site, the largest value for the fd energy difference was found. Also here the highly charged Si^{4+} ions strongly attract the fluoride ion charge clouds. The same was emphasized by van Uitert[19] for complexes like BeF_4^{2-}, AlF_4^-, SiF_6^{2-}, SiO_4^{4-}, and PO_4^{3-} in fluoride and oxide compounds.

The above ideas of attraction of the anion charge cloud by the neighboring small cations can be related to Eq. (4), Eq. (5), and Eq. (3). Charge cloud attraction can be seen as a form of bonding that increases the binding energy of the anion electrons. Stronger binding implies larger oscillation force constant and therewith smaller anion polarizability. According to Eq. (4) smaller centroid shift will result. Stronger binding with other cations than Ce^{3+} will also reduce the covalency between the ligand charge cloud and the $5d$ orbital of Ce^{3+}, i.e., Ce^{3+} ''sees'' a more ionic surrounding. In that case Eq. (5) predicts a smaller centroid shift. Stronger binding lowers the reducing character (electron donating power toward Ce^{3+}) of the oxygen ligands, and this has been the original interpretation of the nephelauxetic series of Eq. (3).

III. DATA ON 5*d*-LEVEL POSITIONS IN FLUORIDE COMPOUNDS

On the scale chosen in Fig. 1 the individual data points belonging to the fluoride compounds are highly overlapping.

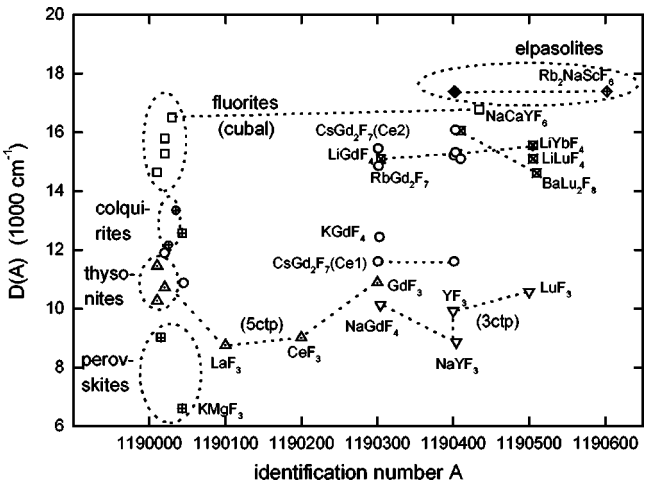

FIG. 2. Spectroscopic redshift in fluoride compounds. Different data symbols were chosen to distinguish different types of compounds. The errors are typically ± 250 cm^{-1}.

The same data are also shown in Fig. 2 where the horizontal scale has been expanded by four orders of magnitude. On this scale the fifth digit of the identification number is significant. It represents the trivalent rare-earth cation that often provides the site for Ce^{3+}. In decreasing order of ionic radius the La, Ce, Gd, Y, Lu(Yb), and Sc containing compounds can be observed from left to right in Fig. 2. For more detailed information on the meaning of the identification number, the reader is referred to Ref. 3. There also information on absorption and emission wavelength, the Stokes shift, and the references to the literature where all information was obtained can be found.

For the interpretation of $D(A)$ also information on ϵ_s, ϵ_c, $\epsilon_{\rm cfs}$ and crystal structure is required. Therefore, all five $5d$-level positions should be known. Such information is only available for a relatively small number of compounds and only if Ce^{3+} is the dopant. Information obtained from literature has been compiled in Table I. Also information was gathered on the crystal structure, in particular, the type of anion polyhedron surrounding the Ce^{3+} site and the point symmetry at that site. References to the literature can be found in the International Crystal Structure Database (ICSD) of FIZ Karlsruhe, Germany. Also the books on inorganic crystal structures by Hyde and Andersson[20] and Wyckoff[21] were frequently consulted.

(N:$R_{\rm av}$) in the second column gives information on the number of anions (N) in the polyhedron and their average distance to the central Ce^{3+} site. $R_{\rm av}$ was determined from crystallographic data. Occasionally it was estimated from an isostructural compound by taking differences in cation ionic radii into account. The shape of the polyhedron and the site symmetry is given in the third column. Information on the polyhedral shapes and their symmetry can be found in the work by Görller-Walrand and Binnemans.[5] Often the polyhedron is not perfectly regular and not all Ce-fluoride distances need to be the same: it results in a lowering of site symmetry. A nearby charge-compensating defect may also lower the symmetry.

Column 4 shows the five wavelengths corresponding to the transitions from the $^2F_{5/2}$ ground state to the five crystal field split $5d$ levels. In $KMgF_3$ at least three different lumi-

TABLE I. Spectroscopic and crystallographic properties of Ce^{3+} doped fluorides. R_{av} is in pm. Type of polyhedron (poly) and point symmetry (sym) at the Ce site are given.

Compound	(N:R_{av})	(poly:sym)	Excitation bands (nm)	ϵ_c(cm^{-1})	ϵ_{cfs} (cm^{-1})	Ref.
free ion			(3×)192, (2×)201	0	2476	2
$KMgF_3$	(12:281)	(cubo:O_h)	203, 210, (??), 227, 234	≈5330	6526	23
$BaLiF_3$	(12:282)	(cubo:C_{4v})	204, 213, 220, 239, 248	6543	8697	27,46
$BaThF_6$	(11:267)	(5ctp:C_2)	188, 206, 220, 238, 256	5576	14129	40
LaF_3	(11:259)	(5ctp:C_2)	194, 208, 218, 234, 249	5580	11386	47,48
CeF_3	(11:257)	(5ctp:C_2)	194, 208, 218, 234, 249	5580	11386	49
$NaYF_4$	(9:≈236)	(3ctp:C_{3h})	196, 207, 221, 233, 247	5630	10535	50
YF_3	(9:232)	(3ctp:C_s)	194, 203, 216, 239, 256	5630	12484	50,51
LuF_3	(9:≈228) [a]	(3ctp:C_s)	191, 202, 214, 232, 259	5130	13746	52
BaF_2	(8:269)	(cubal:C_{3v})	187, 193, 200, (2×)292	6474	19229	53
SrF_2	(9:254)	(1ccubal:C_{4v})	187, 199, 205, (2×)297	7260	19806	53
CaF_2	(9:241)	(1ccubal:C_{4v})	187, 195, 202, (2×)307	7350	20903	28,53
$LiYF_4$	(8:227)	(ddh:S_4)	186, 196, 206, 244, 292	5520	19517	54
$LiLuF_4$	(8:≈224) [b]	(ddh:S_4)	186, 196, 206, 244, 296	5610	19980	55
BaY_2F_8	(8:228)	(ddh:C_2)	188, 197, 212, 244, 300	6143	19858	56,57
$BaLu_2F_8$	(8:≈224) [a]	(ddh:C_1)	183, 196, 225, 246, 288	6130	19923	56
Rb_2NaScF_6	(6:202)	(octa:O_h)	(163, 180), (3×)313	≈8700	≈26500	33
CsY_2F_7:(Ce1)			188, 197, 226, 252, 265	6107	15456	43
CsY_2F_7:(Ce2)			186, 202, 221, 237, 295	6309	19865	43

[a] R_{av} was assumed to be 4 pm smaller than that of the corresponding Y compounds.
[b] R_{av} was assumed to be 0.8 pm smaller than that of $LiYbF_4$.

nescent Ce sites were identified.[22,23] Francini *et al.*,[23] based on work by Ibragimov *et al.*,[24] attribute the dominant Ce^{3+} emission to Ce^{3+} on the 12-fold coordinated K-site with two nearest-neighbor K^+ vacancies for charge compensation. It changes the original O_h symmetry to a site with C_{4v} symmetry. For very low Ce concentration (0.025 mol %) a doublet emission at 263 and 283 nm is observed with excitation bands at 203, 210, 227, and 234 nm. It is attributed by Martini *et al.*[25] and Francini *et al.*[23] to isolated Ce centers on K^+ sites, i.e., without local charge compensation. The data in column 4 pertain to this latter site. The position of the fifth 5d band in $KMgF_3$ is not known and some average was assumed.

For $BaLiF_3$, based on the work by Marsman *et al.*[26] and Yamaga *et al.*,[27] Ce^{3+} is assumed to occupy the Ba^{2+} site with a charge compensating Li^+ on a nearest Ba^{2+} site. It forms a defect with C_{4v} site symmetry. The lowest energy 5d excitation band in the fluorites CaF_2, SrF_2, and BaF_2 was, following the work by Manthey,[28] assumed to be due to the transition to the doublet e_g state. The high-energy 5d levels of Rb_2NaScF_6 are not yet well established: their values have been put within brackets.

Columns 5 and 6 provide ϵ_c and ϵ_{cfs} calculated from the 5d-level positions. The errors in ϵ_c are usually smaller than 100–200 cm^{-1} and ±400 cm^{-1} for ϵ_{cfs}. In cases when 5d levels are not fully certain also ϵ_c and ϵ_{cfs} are more uncertain. Although the structure of CsY_2F_7 is not known, information on the five 5d-level positions of two different Ce sites is compiled.

The energy of the highest 5d level, the centroid position, the energy of the lowest 5d level, and the energy of emission from the relaxed lowest energy 5d level to the $^2F_{5/2}$ ground state are shown in Fig. 3. The energy of emission can be found in Ref. 3. All energies are relative to the centroid position at 51 230 cm^{-1} of the free Ce^{3+} ion. Note the fairly constant centroid shift but widely varying crystal field splitting and Stokes shift ΔS.

IV. DISCUSSION

First the crystal field splitting will be briefly discussed. It will be shown that ϵ_{cfs} is determined by the shape and the size of the coordinating anion polyhedron. A more detailed discussion will be presented in the accompanying paper (Part II). In this part emphasis will be on the interpretation and analyzes of the centroid shift by means of the ligand polar-

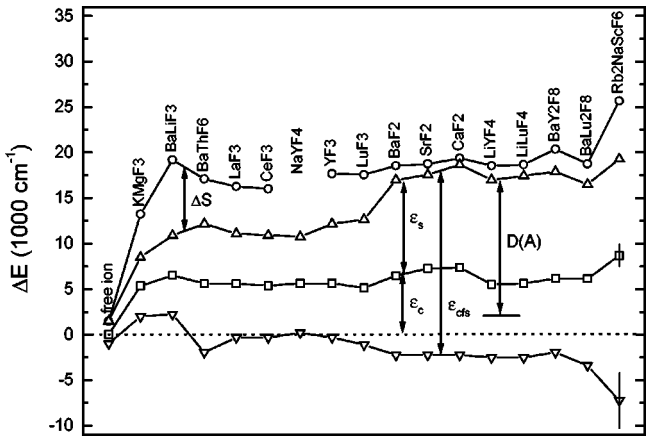

FIG. 3. Energy differences between the centroid position (51,230 cm^{-1}) of the free Ce^{3+} ion and (∇) highest 5d level, (□) centroid position, (△) lowest 5d level, and (○) relaxed lowest 5d level of Ce^{3+} in compounds.

ization model. Both crystal field splitting and centroid shift behave rather independently from one another and in a more or less predictable manner. With the acquired knowledge, finally the redshift in the compounds in Fig. 2 will be interpreted.

A. Crystal field splitting

The crystal field splitting ϵ_{cfs} of the compounds from Table I, more or less arranged in order of decreasing anion coordination number, can be seen in Fig. 3. A first inspection shows that the crystal field splitting tends to increase with decreasing coordination number. The smallest ϵ_{cfs} values are found amongst $KMgF_3$ and $BaLiF_3$. They have the perovskite structure in which the K^+ and Ba^{2+} sites are coordinated by 12 fluoride ions at relatively large distance in the form of a regular cuboctahedron (cubo:O_h).

There are two different Y^{3+} sites in $NaYF_4$ both ninefold coordinated in the form of a trigonal prism with caps on the three rectangular faces.[29] Possibly Ce^{3+} may occupy both sites (R_{av}=233.0 or 238.6 pm) but probably the largest one is preferred. YF_3 and LuF_3 have similar but severely distorted coordination polyhedron. The larger distortion and smaller site size (R_{av}) yield larger crystal field splitting than in $NaYF_4$.

In LaF_3, CeF_3, and $BaThF_6$, which have the hexagonal thysonite structure, the lanthanide ion is 11-fold coordinated with a so-called (distorted) Edshammer polyhedron (see p. 43 in Ref. 20). It resembles a (distorted) tricapped trigonal prism with two more fluoride ions forming caps on the two remaining triangular faces, i.e., a five-capped trigonal prism (5ctp:C_2). Note that these compounds plus those with 3ctp and cuboctahedral coordination all show relatively small crystal field splitting together with large value for the Stokes shift ΔS, see Fig. 3. This anticorrelation has also been observed for several chlorides and oxides.[30]

BaF_2, SrF_2, and CaF_2 have the cubic fluorite structure and the cation has a cubal coordination of eight fluoride ions. The excess charge of the Ce^{3+} ion on the divalent cation site needs to be compensated. In CaF_2 and SrF_2 it is by means of an extra F^- ion preferably located on the nearest interstitial site thus producing a monocapped cube with C_{4v} site symmetry (1ccubal:C_{4v}). In BaF_2 the F^- ion is preferably located at a next-nearest-neighbor site along the (111) direction producing C_{3v} site symmetry. The approximately cubal coordination in BaF_2:Ce^{3+} gives more than a factor of 2 larger ϵ_{cfs} than the cuboctahedral coordination in $BaLiF_3$.

The polyhedron around Y or Lu in the scheelites $LiYF_4$ and $LiLuF_4$, monoclinic BaY_2F_8, and the strongly related structure of orthorhombic[31,32] $BaLu_2F_8$ is a dodecahedron (ddh). All four compounds have about the same R_{av} and show similar crystal field splitting around 20 000 cm^{-1}.

The level positions in the elpasolite Rb_2NaScF_6 were obtained from the work of Aull and Jenssen.[33] The excitation band at 313 nm is assumed to be the triplet component of the octahedrally split $5d$ levels. It is, however, not firmly established whether both the absorption bands observed at 163 and 180 nm are indeed related to the split e_g doublet excitation bands. A conservative estimate for the crystal field splitting caused by the octahedral coordination with relatively short metal-ligand distance is 26 500$\pm$3000 cm^{-1}.

B. Centroid shift

Within the fluorides the centroid shift varies between 5130$\pm$50 cm^{-1} for LuF_3 until 8700$\pm$1200 cm^{-1} for Rb_2NaScF_6. Among the crystals BaF_2, SrF_2, and CaF_2, centroid shift increases with 900 cm^{-1}. At first sight one obvious explanation would be the increasingly smaller site size and hence shorter distance to the fluoride ligands when Ce^{3+} is on the Ba, Sr, or Ca site. However, site size appears not to be the most important parameter that determines the centroid shift. This is demonstrated by LuF_3 which has, despite its relatively small site (9:228) for the large Ce^{3+} ion, the smallest centroid shift of all fluoride compounds. In fact it is the smallest centroid shift of all compounds to be discussed in this and following papers.

It was already noticed by Blasse and Bril,[16] Fouassier *et al.*,[18] and Van Uitert[19] that small highly charged second cations in ternary compounds tend to reduce the redshift. It was explained by the attractive forces of the small cations on the anion charge clouds. Charge is ''pulled'' away from the lanthanide ion located at the large cation site, and interaction between lanthanide $5d$ electrons and anion ligands becomes less. The same idea seems to hold for the centroid shift in binary compounds like YF_3 and LuF_3. The small Y^{3+} ions attract the charge cloud of the fluoride ions more strongly than the 12 pm larger Ce^{3+} ion does. Lu^{3+} is 4 pm smaller than Y^{3+} and an even stronger attractive force is expected. Apparently, despite the smaller site size for Ce^{3+} in LuF_3, its interaction with the F^- $2p$ ligands is less than in YF_3.

Generally one expects that the smaller the ionic radius of the cation and the larger its valency, the more strongly it will attract the fluoride ligands. The decrease of centroid shift in going from $BaLu_2F_8$ to $LiLuF_4$ to LuF_3 provides some indications for the above expectation. The attractive force on the fluoride charge cloud toward the monovalent Li^+ and the large Ba^{2+} are relatively weak compared to that towards Lu^{3+} in LuF_3. The perovskites $KMgF_3$ and $BaLiF_3$ provide even better indications. Two well-resolved excitation bands at 227 nm and 234 nm in $KMgF_3$ are attributed to the split e doublet and a weak band between 200 nm and 215 nm is attributed to the triplet t levels. Although the position of the fifth $5d$ level in $KMgF_3$ is not precisely known, the estimated centroid shift of 5300$\pm$600 cm^{-1} is smaller than that of $BaLiF_3$. Both crystals have the perovskite structure and Ce^{3+} on the K^+ or Ba^{2+} site is in both crystals coordinated by 12 fluoride ions at practically the same distance. The only difference is in the first cation neighbor shell where Mg^{2+} in $KMgF_3$ is thought to yield a stronger attractive force on the fluoride charge cloud than the Li^+ in $BaLiF_3$.

In addition to the attractive forces on the fluoride charge clouds by cations other than Ce^{3+}, also the Ce^{3+} to fluoride ion distances (R_i) and the anion coordination number (N) is of importance for the centroid shift. The model of ligand polarization [see Eq. (4)] and the model of covalency [see Eq. (5)] both predict that the contribution from each fluoride ion to the centroid shift is simply additive. However, the types of cations, the values for R_i, and coordination number differ from compound to compound. This makes it difficult to relate the centroid shift observed for one compound with those of others.

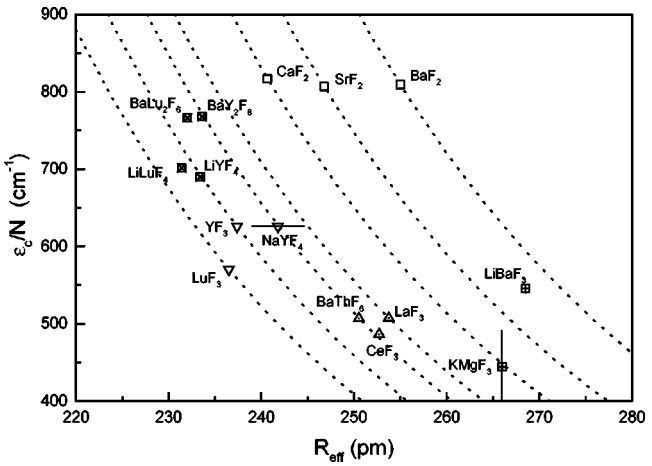

FIG. 4. Centroid shift (ϵ_c) per coordinating (N) fluoride ion. Dashed curves show the dependence on R_{eff}.

To overcome this difficulty, the centroid shift will be further analyzed by using the model of ligand polarization expressed by Eq. (4). The contribution of covalency effects to the centroid will be completely ignored. Following Eq. (4) it will be assumed that (1) the total centroid shift is the result of the added contribution of each coordinating anion individually; (2) only nearest-neighbor anions give a significant contribution to the centroid shift; and (3) all ligands are identical, each with polarizability α_{sp}. Equation (4) can then be rewritten as

$$\frac{\epsilon_c}{N}=\frac{\alpha_{\mathrm{sp}}e^2}{4\pi\epsilon_0}(\langle r^2\rangle_{5d}-\langle r^2\rangle_{4f})\frac{1}{R_{\mathrm{eff}}^6},$$

$$\frac{1}{R_{\mathrm{eff}}^6}\equiv\frac{1}{N}\sum_{i=1}^{N}\frac{1}{(R_i-\frac{1}{2}\Delta R)^6}, \tag{6}$$

where $\frac{1}{2}\Delta R$ has been introduced to account for lattice relaxation around the Ce^{3+} ion. The amount of relaxation is generally not known and as a rough estimation it is assumed that the nearest-neighbor fluoride ions relax radially inward or outward by half the difference ΔR between the ionic radius of Ce^{3+} and the ionic radius of the cation for which it substitutes. For $\langle r^2\rangle_{5d}$ and $\langle r^2\rangle_{4f}$ the values calculated for the free Ce^{3+}, 1.67×10^{-20} m^2 and 0.43×10^{-20} m^2, respectively, were taken.[33,34] Since $\langle r^2\rangle_{5d}$ is considerable larger than $\langle r^2\rangle_{4f}$, the centroid shift is positive as observed experimentally.

R_i was obtained from the crystal structure. ΔR was derived from the effective ionic radii tabulated by Shannon[35] (the so-called crystal radius pertaining to the appropriate coordination number was used). In Fig. 4 the average contribution to the centroid shift from each coordinating fluoride ion ϵ_c/N is shown against R_{eff} as defined in Eq. (6). Through some of the data, the curves representing ϵ_c/N as function of R_{eff} are drawn. The only distinction between the curves is the value for α_{sp} that can be obtained directly with Eq. (6). These values together with those of R_{eff} are compiled in Table II.

α_{sp} appears to behave in a consistent manner with the type of cations present in the structure. The smallest value is observed for LuF_3 and it increases with the ionic radius of the trivalent cation in going to YF_3 and LaF_3. The large divalent cation Ba^{2+} in BaF_2 yields the largest value for α_{sp}. Replacing Ba with the smaller Sr^{2+} or even smaller Ca^{2+} reduces α_{sp} as in SrF_2 and CaF_2. In the series $LiYF_4$, BaY_2F_8, and $NaYF_4$, α_{sp} increases with increasing size and/or decreasing valency of the second cation (Li^+, Ba^{2+}, and Na^+). In the other halides discussed in Part II but particularly the oxides the same trends will be observed.

The assumption that the neighboring ligands relax by half ΔR is of course very crude. If the relaxation were 0.3 or 0.7 times ΔR, and Ce^{3+} substitutes a very small cation like Sc^{3+}

TABLE II. Results from the ligand polarization model. Compounds are arranged according to increase of α_{sp}. α_{exp} are in-crystal fluoride ion polarizabilities derived from macroscopic parameters.

Compound	R_{eff} (pm)	ϵ_c/N (cm^{-1})	α_{sp} (10^{-30} m^3)	α_{exp} (10^{-30} m^3)
LuF_3	237	570	0.69	
$LiLuF_4$	231	701	0.75	
$LiYF_4$	233	690	0.77	
YF_3	237	625	0.78	
$BaLu_2F_8$	232	766	0.83	
BaY_2F_8	234	767	0.87	
$NaYF_4$	242	625	0.87 ± 0.6	
$BaThF_6$	251	506	0.87	
CeF_3	253	487	0.88	
LaF_3	254	507	0.94	
Rb_2NaScF_6	215	1450	0.99 ± 0.14	
$KMgF_3$	266	444	1.09 ± 0.12	0.95 [a]
CaF_2	241	816	1.10	1.06 [b]
SrF_2	247	806	1.26	1.10 [b]
$BaLiF_3$	269	545	1.42	
BaF_2	255	809	1.55	1.15 [b]

[a]Reference 37.
[b]Reference 36.

($\Delta R=-26$ pm) or a very large cation like Ba^{2+} ($\Delta R=+28$ pm), then α_{sp} will change typically by $\pm 10\%$. It may effect slightly the ordering of the compounds as in Table II but the general trend remains the same. Depending whether Ce substitutes the smallest or largest Y site in $NaYF_4$, values of 0.81 and 0.93 are obtained for α_{sp}, respectively. Also accuracy of α_{sp} for Rb_2NaScF_6 and $KMgF_3$ is rather poor because of the uncertainty in ϵ_c. Accuracy of α_{sp} is highest when Ce^{3+} is on a La^{3+} site with negligible $\Delta R=2$ pm.

Instead of using the ligand polarization model, one may also choose to analyze the centroid shift by assuming that it is entirely caused by covalency effects. For that purpose Eq. (5) can be rewritten as

$$\frac{\epsilon_c}{N}=\frac{\beta}{N}\sum_{i=1}^{N} e^{-(R_i-[1/2]\Delta R)/b}, \tag{7}$$

where it is assumed that the overlap integral varies exponentially with the metal to ligand distance[10] and that the term arising from the covalency with the $4f$ orbital can be neglected. Again all N ligands are assumed to be equivalent. With a proper choice of the value for b, the exponential dependence appears quite similar to the power-law dependence of the ligand polarization model. The parameter β should now be seen as a measure for the amount of covalency. Such analyses have been done and about the same ordering of compounds as with the ligand polarization model is obtained.

In-crystal anion polarizabilities cannot be measured directly but have to be inferred, with the help of (empirical or *ab initio*) theoretical models, from macroscopic properties like the dielectric constant or refractory index of the crystals. Values are known for the alkaline earth halides[36] CaF_2, SrF_2, and BaF_2 and the perovskite[37] $KMgF_3$, see Table II. It is reassuring to see that the magnitude of α_{sp} derived from the centroid shift compares so well with experimentally determined fluoride ion polarizabilities. More importantly, theoretical models on anion polarizability predict,[38,39] and it is also observed experimentally, that polarizability decreases when small high valency cations are present in the structure. The (calculated) in crystal fluoride polarizability in the perovskite $KMgF_3$ (0.84×10^{-30} m^3) is smaller than in $KCaF_3$ (0.87×10^{-30} m^3).[37] For the alkali fluorides, the (experimental) polarizability is smallest for LiF (0.80×10^{-30} m^3) and largest for CsF (1.23×10^{-30} m^3), see Ref. 36.

The most appealing aspect of the ligand polarization model is that it is a zero-parameter model, and it provides a direct quantitative and qualitative physical interpretation of the centroid shift. With the covalency model, the interpretation of β and b is much less obvious. Nevertheless a contribution from covalency effects to the centroid shift cannot be ignored and one should regard α_{sp} as a phenomenological parameter representing (1) the effects of ligand polarization, (2) the effects of covalency, and (3) possible charge cloud expansion effects. Since α_{sp} is calculated from the spectroscopic properties, it will hereafter be called the *spectroscopic polarizability*.

C. Spectroscopic redshift $D(A)$

The redshift $D(A)$ of the first $4f\rightarrow5d$ transition of Ce^{3+} in the fluoride compounds is shown in Fig. 2 against the identification number A assigned to the compounds which is treated as a running variable. Figure 2 is a 10 000 times enlarged view of Fig. 1. On this scale, the compounds are grouped depending on the size of rare-earth cations in the structure. Those that do not contain trivalent rare-earth cations have zero value for the fifth digit ($d_5=0$) and they are shown with further expanded horizontal scale in Fig. 5. Yttrium-containing compounds with $d_5=4$ are shown in Fig. 6.

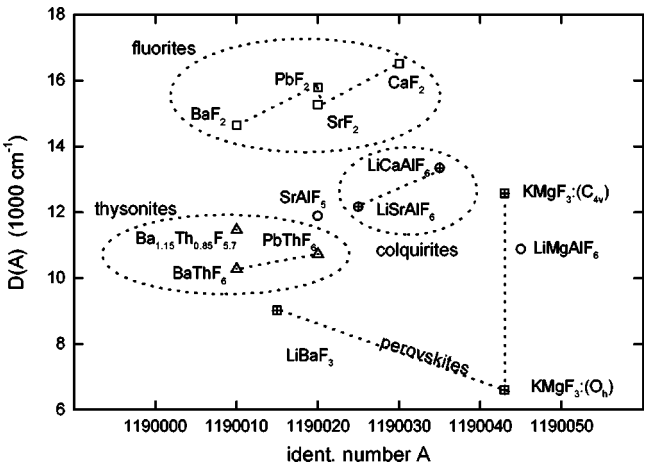

FIG. 5. Spectroscopic redshift in the fluoride compounds with the lanthanide ion on a monovalent or divalent cation site. Different data symbols were chosen to distinguish different types of compounds. The errors are typically ±250 cm^{-1}.

Identification numbers were assigned to the compounds in Ref. 3 in such a way that increase of A tends to reflect increase of the spectroscopic redshift. This can be observed in Fig. 1. It can also be observed in Fig. 2 where the smallest redshift value is found in the left lower corner for the large K^+ site in the perovskite $KMgF_3$ with O_h point symmetry; see also Fig. 5. It is more than 10 000 cm^{-1} larger for the small Sc^{3+} site in the elpasolite Rb_2NaScF_6, see the right top corner of Fig. 2. Figure 3 shows that most of the variation (8000 cm^{-1}) in the redshift stems from variations in the crystal field splitting. The variation in the centroid shift is two times smaller.

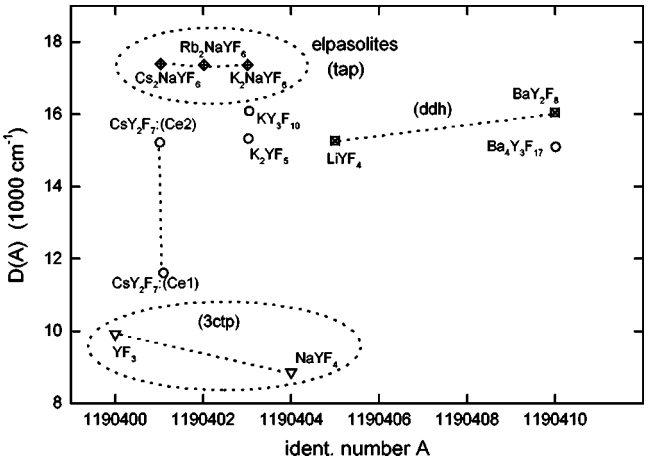

FIG. 6. Spectroscopic redshift in the yttrium-based fluoride compounds. Different data symbols were chosen to distinguish different types of compounds. The errors are typically ±250 cm^{-1}.

Going from small to large $D(A)$ in Fig. 2, one first encounters the perovskites and next the compounds with coordination in the form of a five-capped (5ctp) or a tricapped trigonal prism (3ctp). The larger redshift of the thysonite GdF_3 as compared to LaF_3 (11:259) and CeF_3 (11:257) is attributed to increase of crystal field splitting. $PbThF_6$ and $BaThF_6$ have also the thysonite crystal structure, see Fig. 5, but with a random distribution of the two cations over the available sites and somewhat larger, 1% and 3%, respectively, lattice parameters[40,41] than LaF_3. Redshift in these compounds is 2000 cm^{-1} larger than in LaF_3. Redshift is even larger in $Ba_{1.15}Th_{0.85}F_{5.7}$, which has, compared to $BaThF_6$, a fluoride ion deficiency resulting into fluoride vacancies in the coordination polyhedron. Probably the missing fluoride ion enhances the otherwise small crystal field splitting. Tricapped trigonal prismlike coordination is found in $NaGdF_4$ (9:≈239), $NaYF_4$, YF_3, and LuF_3. All compounds show small redshift attributed to small crystal field splitting. The above data show that type and size of the anion coordination polyhedron around Ce^{3+} are crucial for the crystal field splitting and redshift.

Moving toward larger $D(A)$ values one arrives at compounds with eightfold coordination, the fluorites BaF_2 (8:269), PbF_2 (8:257), SrF_2 (8:250), and CaF_2 (8:237), the scheelites $LiGdF_4$, $LiYF_4$, $LiYbF_4$, $LiLuF_4$, and the compounds BaY_2F_8 and $BaLu_2F_8$. Most of them were already discussed in Secs. IV A and IV B. Note the tending increase of redshift in the fluorites, see Fig. 5, with decrease of the size of the coordinating cubal polyhedron.

$NaCaYF_6$ (8:236) has the same structure as CaF_2 but with a random distribution of the three cations over the available sites. Redshift is practically the same as in CaF_2; see Fig. 2. KY_3F_{10} is a so-called anion excess fluorite.[42] The lanthanide site is coordinated by eight-fluoride ions in the form of a square antiprism. The point charge electrostatic model predicts that the crystal field splitting for the antiprism is quite similar to that of the normal prism, see Part II and Ref. 5. The yttrium site in $Ba_4Y_3F_{17}$, see Fig. 6, is coordinated by a monocapped square antiprism.

The crystal structure of the crystallographically related compounds $RbGd_2F_7$, $CsGd_2F_7$, and CsY_2F_7 is not precisely known. Two different luminescing Ce sites were observed in the last two compounds.[43] The data on CsY_2F_7, see Table I, show that the crystal field splitting at both sites is different resulting in different redshift, see Fig. 2.

The largest redshifts are found among the cubic elpasolites M_2NaYF_6 (M=Cs,Rb,K) and Rb_2NaScF_6 with the sixfold coordinated rare-earth sites. The luminescence properties of the yttrium-based elpasolites are quite complicated because there appear to be different luminescing sites.[33] The dominating emission stems from Ce^{3+} on the octahedrally sixfold coordinated Y site, the so-called blue emission.[33] It is characterized by a large redshift and hence long absorption and emission wavelengths. Starting with Cs_2NaYF_6 (6:227) via Rb_2NaYF_6 (6:217) to K_2NaYF_6 (6:213), see Fig. 6, the site size decreases but $D(A)$ remains practically constant. Rb_2NaScF_6 (6:202) despite its very small site size has only slightly larger redshift than Rb_2NaYF_6.

The above results show that in the fluorides the coordination number is important for the overall redshift. It determines the crystal field splitting, which is the dominant contribution to the redshift. Coordination number depends on the size of the cation that is being replaced by Ce^{3+} but also on the size of other cations in the crystal. This can be demonstrated with the yttrium-based fluorides in Fig. 6. Decrease of coordination number around the yttrium ion can be accomplished by introducing large cations and/or lower valency cations into the structure. YF_3 has ninefold coordination; replacing part of the Y ions with larger Ba^{2+} or K^+ ions results in BaY_2F_8, KY_3F_{10}, and KY_2F_7 each with eightfold coordination. In K_2YF_5 (7:224) where the abundance of large K ions is relatively large the coordination is reduced to sevenfold. In the elpasolites with several large cations, the coordination is even reduced to sixfold.

The reason for these coordination changes is purely crystallographic in origin. Large cations like K^+, Cs^+, Ba^{2+} require a large coordination number of anions (N=10–12) and this goes at the expense of the coordination around the smaller lanthanides, i.e., in this case the yttrium ions. Monovalent cations like Li^+ in $LiYF_4$ also enhance the cation to anion ratio, which also tends to reduce the coordination number around the yttrium ion. The same behavior can be observed in Fig. 2 for the Gd- and the Lu-based fluorides.

The reverse behavior is expected if small cations like B^{3+}, Si^{4+}, or Al^{3+} are introduced into the structure. These ions require a small coordination number (N=4–6) resulting in an enhancement of the coordination number around the large lanthanide ion. This can be demonstrated by Fig. 5. The coordination in CaF_2 (8:237) and SrF_2 (8:250) is eightfold. In the colquirites $LiCaAlF_6$ and $LiSrAlF_6$ the coordination around the M^{2+} site is 12-fold of which six fluoride ions are located at relatively close distance of 228 pm and 242 pm, respectively, and six at large distance of 349 pm and 353 pm, respectively. In $SrAlF_5$ the coordination is even 13- to 14-fold. Figure 5 shows that redshift becomes increasingly smaller. The small cations enhance coordination number and therewith tend to reduce the crystal field splitting. They also reduce the polarizability of the fluoride ligands thus reducing the centroid shift as expressed in Eq. (6).

D. The role of charge compensating defects

The necessity of charge compensation is often a complicating factor in the interpretation of the redshift of compounds where the lanthanide ion occupies a divalent cation site and especially a monovalent cation site. In CaF_2 compensation is by means of a fluoride ion at the nearest interstitial site. If treated in oxygen atmosphere an O^{2-} ion may substitute for a nearest fluoride ion as the charge compensator. The zero phonon absorption line measured at low temperature shifts by 2300 cm^{-1} from 313.2 to 338 nm.[28] The polarizability of the O^{2-} ion in CaO amounts[38] to 2.38 $\times 10^{-30}$ m^3, which is more than two times larger than that of F^- in CaF_2. Also covalency between O^{2-} and Ce^{3+} will be larger than in the case of F^-. One therefore expects a substantial enhancement of the centroid shift.

Possibly charge compensating oxygen ions play also a role in $NaF:Ce^{3+}$ (6:231). The work by Pisarenko *et al.*[44,45] yields a redshift of 23 700 cm^{-1}, which is exceptionally large for a fluoride compound; see Fig. 1. Assuming a crystal field splitting of at most 27 000 cm^{-1}, i.e., about the same largeness as in Rb_2NaScF_6, one obtains with Eq. (2) and

$r(A) \approx 2$ a centroid shift of around 12 500 cm^{-1}. This is too large for a fluoride compound and clearly something must have changed in the structure. Pisarenko *et al.* suggest the presence of Na vacancies as charge compensator. However, this cannot explain the large centroid shift and redshift. One may speculate on the presence of two oxygen ions at neighboring fluoride sites. They may contribute 7000 cm^{-1} to the total centroid shift. If so, NaF:Ce should be treated as a fluoro-oxide compound instead of a fluoride compound.

V. SUMMARY AND CONCLUSIONS

Data have been collected on $5d$-level positions of Ce^{3+} in fluoride crystals from which the values for the centroid shift ϵ_c, crystal field splitting ϵ_{cfs}, and redshift $D(A)$ were obtained. ϵ_{cfs} is determined by the type and size of the anion polyhedron coordinating the Ce^{3+} ion. Cuboctahedral, five-capped, and tricapped trigonal prism coordination always appear to produce small crystal field splitting with large values for the Stokes shift. Cubal and octahedral type coordination yield 2 to 3 times larger crystal field splitting but much smaller Stokes shift.

With the ligand polarization model, the so-called spectroscopic polarizability (α_{sp}) has been introduced that is obtained from the observed centroid shift without the use of any fitting parameters. Its value increases in a systematic manner with increasing size and decreasing valency of the cations in the structure. The value for α_{sp} and its dependence on the type of cations in the structure behave qualitatively and quantitatively similar to experimentally known polarizabilities of the fluoride ions. Small highly charged cations reduce α_{sp} and α_{exp}: large cations have the opposite effect.

In order of decreasing importance three aspects determine the spectroscopic redshift of the first allowed fd transition: (1) the type of anion coordination polyhedron, (2) the size of the cation that is replaced by Ce^{3+}, and (3) the attractive forces on the fluoride charge clouds by the cations other than Ce^{3+}.

[1] P. Dorenbos, J. Lumin. **91**, 91 (2000).
[2] R.J. Lang, Can. J. Res. **14**, 127 (1936).
[3] P. Dorenbos, J. Lumin. **91**, 155 (2000).
[4] J.S. Griffith, *The Theory of Transition-Metal Ions* (Cambridge University Press, London, 1961).
[5] C. Görller-Walrand and K. Binnemans, in *Handbook on the Physics and Chemistry of Rare Earths*, edited by K.A. Gschneidner, Jr. and L. Eyring (Elsevier Science B.V., Amsterdam, 1996), Vol. 23, Chap. 155.
[6] M. Faucher and D. Garcia, Phys. Rev. B **26**, 5451 (1982).
[7] C.K. Jörgensen, *Modern Aspects of Ligand Field Theory* (North-Holland, Amsterdam, 1971).
[8] S. Sugano and R.G. Shulman, Phys. Rev. **130**, 517 (1963).
[9] C.A. Morrison, J. Chem. Phys. **72**, 1001 (1980).
[10] B.F. Aull and H.P. Jenssen, Phys. Rev. B **34**, 6640 (1986).
[11] R.G. Denning, A.J. Berry, and C.S. McCaw, Phys. Rev. B **57**, R2021 (1998).
[12] J.D. Axe and G. Burns, Phys. Rev. **152**, 331 (1966).
[13] P. Caro and J. Derouet, Bull. Soc. Chim. Fr. **1**, 46 (1972).
[14] P. Caro, O. Beaury, and E. Antic, J. Phys. (France) **37**, 671 (1976).
[15] E. Antic-Fidancev, M. Lemaitre-Blaise, and P. Caro, New J. Chem. **11**, 467 (1987).
[16] G. Blasse and A. Bril, Philips Res. Rep. **22**, 481 (1967).
[17] G. Blasse and A. Bril, J. Chem. Phys. **47**, 5139 (1967).
[18] C. Fouassier, B. Latourette, J. Portier, and P. Hagenmuller, Mater. Res. Bull. **11**, 933 (1976).
[19] L.G. van Uitert, J. Lumin. **29**, 1 (1984).
[20] B.G. Hyde and S. Andersson, *Inorganic Crystal Structures* (Wiley, New York, 1989).
[21] R.W.G. Wyckoff, *Crystal Structures* (Wiley, New York, 1963), Vols. 1 and 2.
[22] A. Gektin, V. Komar, V. Shlyahturov, and N. Shiran, IEEE Trans. Nucl. Sci. **43**, 1295 (1996).
[23] R. Francini, U.M. Grassano, L. Landi, A. Scacco, M. D'Elena, M. Nikl, N. Cechova, and N. Zema, Phys. Rev. B **56**, 15 109 (1997).
[24] I.R. Ibragimov, I.I. Fazlizhanov, M.L. Falin, and V.A. Ulanov, Fiz. Tverd. Tela (Leningrad) **34**, 3261 1992) [Sov. Phys. Solid State **34**, 1745 (1992)].
[25] M. Martini, F. Meinardi, and A. Scacco, Chem. Phys. Lett. **293**, 43 (1998).
[26] M. Marsman, H. Andriessen, and C.W.E. van Eijk, Phys. Rev. B **61**, 16 477 (2000).
[27] M. Yamaga, T. Imai, K. Shimamura, T. Fukuda, and M. Honda, J. Phys.: Condens. Matter **12**, 3431 (2000).
[28] W.J. Manthey, Phys. Rev. B **8**, 4086 (1973).
[29] M.F. Joubert, C. Linares, B. Jacquier, A. Cassanho, and H.P. Jenssen, J. Lumin. **51**, 175 (1992).
[30] P. Dorenbos, J. Andriessen, M. Marsman, and C.W.E. van Eijk, Radiat. Eff. Defects Solids (to be published).
[31] N.L. Tkachenko, L.S. Garashina, O.E. Izotova, V.B. Aleksandrov, and B.P. Sobolev, J. Solid State Chem. **8**, 213 (1973).
[32] B.P. Sobolev and N.L. Tkachenko, J. Less-Common Met. **85**, 155 (1982).
[33] B.F. Aull and H.P. Jenssen, Phys. Rev. B **34**, 6647 (1986).
[34] J. Andriessen (private communication).
[35] R.D. Shannon, Acta Crystallogr., Sect. A: Cryst. Phys., Diffr., Theor. Gen. Crystallogr. **32**, 751 (1976).
[36] E.W. Pearson, M.D. Jackson, and R.C. Gordon, J. Phys. Chem. **99**, 119 (1984).
[37] P.W. Fowler, F. Ding, and R.W. Munn, Mol. Phys. **84**, 787 (1995).
[38] P.W. Fowler and P.A. Madden, J. Phys. Chem. **89**, 2581 (1985).
[39] A. Batana, J. Bruno, and R.W. Munn, Mol. Phys. **92**, 1029 (1997).
[40] P. Mesnard, Ph.D. thesis, University of Bordeaux, France 1997.
[41] P. Mesnard, A. Garcia, J. Grannec, C. Fouassier, D. Bouttet, and C. Pedrini, Chem. Phys. Lett. **229**, 139 (1994).
[42] Y. Le Fur and S. Aleonard, J. Solid State Chem. **95**, 403 (1991).
[43] D.R. Schaart, P. Dorenbos, C.W.E. van Eijk, R. Visser, C. Pedrini, B. Moine, and N.M. Khaidukov, J. Phys.: Condens. Matter **7**, 3063 (1995).
[44] V.F. Pisarenko, G.D. Potapenko, and V.V. Popov, Opt. Spectrosc. **38**, 93 (1975) [Opt. Spectrosc. **38**, 51 (1975)].
[45] V.F. Pisarenko, G.D. Potapenko, and V.V. Popov, Opt. Spek-

trosk. **39**, 915 (1975) [Opt. Spectrosc. **39**, 522 (1975)].
[46] C.M. Combes, P. Dorenbos, C.W.E. van Eijk, J.Y. Gesland, and P.A. Rodnyi, J. Lumin. **72-74**, 753 (1997).
[47] K.H. Yang and J.A. DeLuca, Appl. Phys. Lett. **31**, 499 (1976).
[48] A.J. Wojtowicz, M. Balcerzyk, E. Berman, and A. Lempicki, Phys. Rev. B **49**, 14 880 (1994).
[49] C. Dujardin, C. Pedrini, N. Garnier, A.N. Belsky, K. Lebbou, and T. Fukuda, Opt. Mater. (to be published).
[50] J.C. Krupa, M. Queffelec, N.Y. Kirikova, and V.N. Makhov, Mater. Sci. Forum **315–317**, 27 (1999).
[51] M. Domineé-Bergès and J. Loriers, Acad. Sci., Paris, C. R. **301-II**, 915 (1985).
[52] K.H. Yang and J.A. DeLuca, Appl. Phys. Lett. **35**, 301 (1979).
[53] E. Loh, Phys. Rev. **154**, 270 (1967).
[54] C.M. Combes, P. Dorenbos, C.W.E. van Eijk, C. Pedrini, H.W. den Hartog, J.Y. Gesland, and P.A. Rodnyi, J. Lumin. **71**, 65 (1997).
[55] C.M. Combes, Ph.D. thesis, Delft University of Technology, The Netherlands, 1999.
[56] J.C. van't Spijker, P. Dorenbos, C.W.E. van Eijk, J.E.M. Jacobs, H.W. den Hartog, and N. Korolev, J. Lumin. **85**, 11 (1999).
[57] S.P. Chernov, L.I. Devyatkova, O.N. Ivanova, A.A. Kaminskii, V.V. Mikhailin, S.N. Rudnev, and T.V. Uvarova, Phys. Status Solidi A **88**, K169 (1985).